Positron spin-relaxation (μ^+SR) study of carbon phases, SiC, and fused quartz

1998 J. Phys.: Condens. Matter 10 10493

(http://iopscience.iop.org/0953-8984/10/46/016)

J. Phys.: Condens. Matter **10** (1998) 10493–10506. Printed in the UK PII: S0953-8984(98)97375-1

Positron spin-relaxation (e^+SR) study of carbon phases, SiC, and fused quartz

Th Gessmann, J Major† and A Seeger

Max-Planck-Institut für Metallforschung, Heisenbergstrasse 1, D-70569 Stuttgart, Germany, and Universität Stuttgart, Institut für Theoretische und Angewandte Physik, Pfaffenwaldring 57, D-70569 Stuttgart, Germany

Received 30 April 1998

Abstract. The positron spin-relaxation (e^+SR) method permits the detection and investigation of positronium (Ps) in condensed matter with very small formation probabilities. In a set-up that makes use of spin-polarized positrons emitted from a $^{68}Ge/^{68}Ga$ source, the effect of reversals of an external magnetic field applied longitudinally to the positron spin polarization on the Doppler broadening of the annihilation photon line is measured. For the first time, the fractions r of Ps-forming positrons and normalized electron densities κ at the positron in Ps have been determined for natural type-IIa diamond ($r = 0.07, \kappa = 1$) and crystalline SiC ($r = 0.04, \kappa = 0.15$). The two materials show a hitherto not observed anomalous dependence of the Doppler broadening on the magnetic field strength that indicates that a large Ps fraction annihilates before becoming thermalized. Fused quartz ($r = 0.67, \kappa = 1.4$), C_{60} fullerite ($r = 0.03, \kappa = 0.3$), and highly orientated pyrolytic graphite ($r = 0.01, \kappa = 0.7$) showed the 'normal' field dependence.

1. Introduction

Owing to the non-conservation of parity in β-decay, positrons (e^+) emitted from radioactive sources are spin polarized. The measure of the spin polarization of spin-1/2 particles, the *helicity* $\mathcal{H}$, is defined as the expectation value of the projection of the spin, $\boldsymbol{s}$, measured in units of $\hbar/2$ ($h = 2\pi\hbar$ = Planck's constant), onto the direction of the particle momentum, $\boldsymbol{p}$. For positrons emitted from radioactive sources with speed v, the helicity is given by

$$\mathcal{H} = v/c \tag{1}$$

where c denotes the speed of light. Although the spectrum average of the helicity, $\langle\mathcal{H}\rangle$, can be quite large (in the present experiments $\langle\mathcal{H}\rangle = 0.92$; cf. section 3), in condensed-matter studies employing positrons rather little use is being made of the e^+ spin polarization. This is in striking contrast to the flourishing and rapidly expanding applications of low-energy positive muons (μ^+) [1–3], which are almost entirely based on the spin polarization of muons obtained from the semi-leptonic decay of π-mesons.

In the present context, the most important difference between μ^+ and e^+ is that positive muons *decay* into positrons and two neutrinos through the weak interaction and therefore under non-conservation of parity, whereas positrons *annihilate* with electrons (e^-) through the parity-conserving electromagnetic interaction. In the first case the direction of the e^+ emission is correlated with the spin directions of the decaying muons. This allows us to obtain information on the spin polarization at the moment of decay and, thus, through the

† Author to whom any correspondence should be addressed.

0953-8984/98/4610493+14$19.50

coupling of spin and magnetic moment, on the 'magnetic history' of an ensemble of spin-polarized μ^+ implanted into matter. In marked contrast to this, the dominant annihilation mode of e^+ in condensed matter, namely the collinear emission of two 511 keV photons (γ-quanta), is always isotropic. Nevertheless, in certain circumstances information on the e^+ spin polarization *can* be obtained from 2γ-annihilation due to the fundamental difference between *annihilation* and *decay*. While the μ^+-decay is not influenced by the environment (as a consequence, the mean lifetime of μ^+ is invariably equal to $\tau_\mu = 2.2\ \mu$s), this is expressly not so for the e^+e^- annihilation. The rate of annihilation (=the inverse of the positron lifetime) is proportional to the overlap of the e^+ wavefunction with the wavefunctions of the electrons with spins antiparallel to the e^+ spin and thus dependent not only on the annihilation site but also on the spin polarization of the electrons at that site.

A further source of information is a consequence of the fact that the above-mentioned collinearity of the photons resulting from the 2γ-annihilation of positron–electron pairs holds in the *rest system* of the annihilating pair but *not* necessarily in the *laboratory system*. Only if the pair momentum is negligibly small compared to $m_e c$ (m_e = electron mass), as it is in the case of the annihilation of the e^+ in *thermalized* parapositronium (p-Ps) with their 'own' electrons (in the following called self-annihilation), is the emission of *all* photon pairs collinear in the laboratory system as well. If, however, at the time of their annihilation the p-Ps 'atoms' still possess an appreciable momentum transverse to the direction in which the 2γ-emission is observed, i.e. if their slowing down is delayed on the timescale of their lifetime, the 2γ-emission is no longer collinear in the laboratory system. At the same time, the annihilation photons are Doppler shifted by

$$\Delta E_\gamma = \pm c p_l/2 \tag{2}$$

where p_l denotes the component of the pair momentum in the direction of observation. (Occasionally, p_l will be referred to as 'longitudinal momentum'.)

Since experimental and theoretical evidence strongly indicates that e^+ *not* bound in Ps ($=e^+e^-$) virtually always thermalize within times that are short compared to their lifetimes [4–6], the phenomenon just described allows us to detect the momentum distribution of non-thermalized p-Ps by means of ACAR (angular correlation of annihilation radiation) or Doppler broadening (ΔE_γ) measurements. In general, the information that may be obtained by measuring the angular correlation curve or the Doppler broadening of the 511 keV photon line is independent of the direction of the positron spins and thus of the e^+ spin polarization. There are two important exceptions, however, both of which are direct consequences of the fact that 2γ-annihilation is possible only if the two partners of the annihilating pair have opposite spins.

(i) If a fraction of the participating *electrons* are spin polarized, reversal of the positron spins changes the density and the momentum distribution of the electrons available for annihilation [7].

(ii) *Self-annihilation of positronium* takes place only in the 1^1S_0 (singlet) state (e^+ and e^- spins antiparallel) but not in the 1^3S_1 (triplet) state (e^+ and e^- spins parallel). (We are justified in confining the discussion to the 1S states.) External magnetic fields mix these states and thus alter the annihilation rates; the energy eigenstate in the presence of external magnetic fields emerging from 1^1S_0 (=parapositronium) is called plesio-parapositronium (pp-Ps), the eigenstate emerging from 1^3S_1 (=orthopositronium) is called meiktopositronium (m-Ps) [8]. The occupancy of the 'mixed' states depends on the spin polarization of the positrons. As the present work demonstrates, spin-polarized positrons provide us with a very powerful tool for the study of Ps formation.

Both possibilities for utilizing the e^+ spin polarization, a 'free gift' from Mother Nature, require fairly large external magnetic fields along the spin-polarization axis. Since it would usually be rather impractical to reverse the direction of the e^+ polarization, most experiments are performed by reversing the external magnetic field.

Notwithstanding the differences mentioned above, the techniques allowing us to exploit the e^+ spin polarization are similar to the study of positive muons by means of the muon spin relaxation in a *longitudinal* (with respect to the polarization direction) magnetic field, one of the basic μSR techniques [1]. Because of this analogy, the present technique has been dubbed e^+SR [9, 10]. An important difference between e^+SR and longitudinal μSR is that, in contrast to μSR, in typical e^+SR measurements the sample to be investigated must serve also as detector for the relaxation of the spin polarization. For this reason the range of applicability of e^+SR is much narrower than that of μSR.

e^+SR detectors according to alternative (i) may be ferromagnets alternately magnetized parallel and antiparallel to the e^+ polarization [10, 11]; here the e^+ spin polarization 'relaxes' (i.e. tends towards its equilibrium value) provided that the magnetic moments of the positrons interact with varying internal magnetic fields perpendicular to the e^+ spin direction. Materials containing paramagnetic trapping centres permit e^+SR measurements by reversing the sample magnetization, too. In this case, however, a sufficiently strong magnetization can only be achieved by applying large magnetic fields at quite low temperatures; as an example we mention a recent study of 'paramagnetic' electrons in F centres in KCl [12].

Use of alternative (ii) is made in studies of Ps by e^+SR. Here the spin relaxation is due to the hyperfine interaction between the magnetic moments of positrons and electrons bound in Ps. The determination of the helicity of positrons from ^{22}Na by the e^+SR technique provided the first demonstration that positrons emitted by unpolarized radioactive sources are longitudinally spin polarized [13]. In some molecular substances e^+SR measurements revealed positron spin relaxation during the slowing-down process of the positrons [14, 15]. For overviews regarding item (ii) and additional references see [16, 17].

The present paper reports and discusses e^+SR studies of Ps formation in natural type-IIa diamond, crystalline SiC, fused quartz, graphite, and C_{60} fullerite (section 4 and 5). Section 3 gives a brief description of the experimental set-up and extends the formerly described data analysis [18] to include the formation of *non-thermalized* positronium. A quantitative model for the slowing-down process of Ps in condensed matter [19] is reviewed in section 2.1; the eigenstates of the spin Hamiltonian of positronium in external magnetic fields are discussed in section 2.2 (for a more detailed account see [8]).

2. Theoretical background

2.1. Slowing down of Ps

The kinetic energies of positrons implanted into condensed matter are much larger than the thermal equilibrium value $3k_BT/2$, where k_B denotes Boltzmann's constant and T the absolute temperature. Most of the kinetic energy is lost rather rapidly by energy transfer to the host material, the creation of electron–hole pairs and the inelastic scattering of positrons by phonons being the main processes responsible for the slowing down of e^+ in condensed matter [20]. The excitation of phonons becomes effective only when the kinetic energies of the positrons are comparable to the maximum phonon energies. Multi-phonon processes contribute only little to the slowing down of e^+.

Ps forms in general with kinetic energies E_{kin} that are large compared to $3k_BT/2$. Because of its charge neutrality, Ps cannot create electron–hole pairs; therefore the excess

kinetic energy has to be dissipated by inelastic Ps–phonon interactions. In materials with optical phonon branches this will predominantly occur by the excitation of optical phonons, since their energies $\hbar\omega_{\mathrm{op}}$ and their densities of states are larger than those of acoustic phonons. The prediction that in Ps-forming materials *without* optical phonon branches the slowing down of Ps should be delayed has been verified by measurements on the solid rare gases Ne, Ar, and Kr [21].

A quantitative model for the inelastic scattering of light 'particles' such as Ps by optical phonons [19] predicts that as long as

$$E_{\mathrm{kin}} \gg \hbar\omega_{\mathrm{op}}\,\mathrm{cotanh}(\hbar\omega_{\mathrm{op}}/2k_{\mathrm{B}}T)/2 \tag{3}$$

holds, the particle momentum decreases linearly with time according to

$$p(t) = p_0\left(1 - \frac{t}{\tau_{\mathrm{sd}}}\right). \tag{4}$$

Here p_0 is the initial momentum and

$$\tau_{\mathrm{sd}} = 2\pi\rho p_0(\hbar/mE_{\mathrm{op}})^2 \tag{5}$$

the slowing-down time. In (5), m denotes the particle mass (in the case of Ps, $m = 2m_{\mathrm{e}}$), E_{op} a deformation 'potential' with the dimension of a force, and ρ the density of the host material. The independence of τ_{sd} of T and ω_{op} is a consequence of the condition (3).

2.2. Ps spin eigenstates and e^+ spin polarization

As mentioned in section 1, the study of Ps by the e^+SR technique rests on the 'mixing' of the zero-field eigenstates of the spin Hamiltonian by an applied magnetic field $\boldsymbol{B}$. In the absence of an external magnetic field the spin eigenstates of Ps may be characterized by the symbol $|S, m\rangle$, where S denotes the quantum number of the total spin and m the 'magnetic' quantum number. In this notation p-Ps has the spin eigenvector $|0, 0\rangle$; the three energetically degenerate spin states of o-Ps are characterized by $|1, 1\rangle$, $|1, 0\rangle$, and $|1, -1\rangle$. Since in a magnetic field m remains a 'good' quantum number (in contrast to S), the states $|1, 1\rangle$ and $|1, -1\rangle$ are not affected by the magnetic field and retain therefore the properties of o-Ps. In the following they will be denoted by the labels $j = 3$, 4. Of the two $m = 0$ states in a magnetic field, the pp-Ps state (reducing to $|0, 0\rangle$ for $B \longrightarrow 0$) will be denoted by $j = 1$, and m-Ps, the state that reduces to $|1, 0\rangle$ for $B \longrightarrow 0$, will be denoted by $j = 2$. In the data analysis we also have to take into account the annihilation of e^+ not bound in Ps (so-called free e^+); to them the label $j = 0$ is assigned.

Several processes may contribute to the dependence of the population numbers $n_j(t)$ ($j = 0$, 1, 2, 3, 4) of the five states introduced in the preceding paragraph on the *age* t (=time passed since Ps formation).

(i) e^+ *annihilation*. The magnetic fields achievable in the laboratory are too weak to influence the annihilation process *per se*. This means that in our analysis only 2γ-annihilation needs to be taken into account, that self-annihilation affects only the $|0, 0\rangle$ contributions to the two $m = 0$ states (in a $\boldsymbol{B}$-dependent manner), and that the rate of the pick-off annihilation (=annihilation of the e^+ in Ps with a 'foreign' electron of opposite spin, thus reflecting the momentum distribution of the electrons at the Ps location) is $\boldsymbol{B}$-independent.

(ii) *Spin exchange*. The exchange of spin directions between 'foreign' electrons and the electrons bound in Ps (the analogue of the 'flip-flop processes' well known in magnetic resonance) transforms $S = 1$ states into $S = 0$ states and vice versa.

(iii) *Positronium inhibition*. Oxidizing substances such as $K_2S_2O_8$ may grasp the e^- from Ps and thus turn Ps into free e^+ [22]. A detectable age dependence of the occupation numbers may result if this process is diffusion controlled [23].

The rate equations describing the processes (i) and (ii) have been formulated and extensively discussed elsewhere (see, e.g., [8]). (Process (iii) could be easily incorporated but is unimportant in the present work.) If r denotes the fraction of implanted e^+ that form positronium instantaneously and $\mathcal{P}$ the spin polarization of the implanted e^+, the initial conditions read

$$n_0(0) = 1 - r \tag{6a}$$

$$n_1(0) = (r/4)\,[1 + x\mathcal{P}(1 - 2\zeta)] \qquad n_2(0) = (r/4)\,[1 - x\mathcal{P}(1 - 2\zeta)] \tag{6b}$$

$$n_3(0) = (r/4)(1 + \mathcal{P}) \qquad n_4(0) = (r/4)(1 - \mathcal{P}). \tag{6c}$$

The dimensionless coefficient

$$\zeta := [1 - (1 + x^2)^{-1/2}]/2 \tag{7}$$

appearing in (6) depends on the normalized magnetic field

$$x = 4\mu_e B/\Delta E^{hf} = \kappa^{-1} B/3.63\ \mathrm{T} \tag{8}$$

where $\Delta E^{hf} = \kappa \times 0.8412$ meV denotes the Ps hyperfine splitting in matter and $\mu_e = 5.795 \times 10^{-5}$ eV T^{-1} the electron magnetic moment. The dimensionless parameter κ is defined as the electron density at the e^+ site in Ps divided by its vacuum value [24, 25]; thus κ equals unity in vacuum. $\mathcal{P}$ denotes the spin polarization of the e^+ ensemble whose annihilation is investigated. In common with the helicity $\mathcal{H}$, $\mathcal{P}$ is a pseudoscalar quantity. It is defined as the expectation value of the normalized projection of the spins $\boldsymbol{s}$ onto a *fixed* space direction $\boldsymbol{r}^0$, and *not*, like $\mathcal{H}$, with respect to the *momentum* direction of the positrons. This has the consequence that

$$\mathcal{P} = \langle \boldsymbol{s} \cdot \boldsymbol{r}^0 \rangle / s \tag{9}$$

may be different from zero even for slowed-down e^+, whereas $\mathcal{H}$ loses its meaning for particles at rest.

The slowing down of e^+ in condensed matter is so fast that the polarization of an implanted beam of e^+ is preserved to a high degree†. If Ps is formed, this need not be true, since the slowing-down time of Ps may not be negligibly small compared to the inverse of the hyperfine frequency $\nu^{hf} = \Delta E^{hf}/h = \kappa \times 2.03 \times 10^{11}\ s^{-1}$, which is a measure of the spin-flip rate in Ps. As will be seen in section 4, non-thermalized p-Ps may indeed leave a clear mark in the e^+SR data.

Equations (6*a*)–(6*c*) have been normalized according to

$$\sum_{j=0}^{4} n_j(0) = 1. \tag{10}$$

Since our experimental set-up integrates over the e^+ age, we do not require the explicit solutions $n_j(t)$. Rather, the various annihilation fractions I_l (the so-called intensities), where the subscript l stands for p-Ps (=annihilation with the characteristics of p-Ps, whether

† The discovery that even slow positrons emitted from certain moderators are still polarized [26] initiated the production of spin-polarized positron beams. Such beams may serve, e.g., as probes of surface magnetism by investigating Ps formation at the surface [27]; other applications may be found in [28].

thermalized or not), po (=pick-off annihilation), or f (=annihilation of free e^+), are directly related to the time integrals of the occupation numbers

$$\mathcal{L}_j(0) = \int_0^\infty n_j(t)\ \mathrm{d}t \qquad (j = 0, 1, 2, 3, 4) \tag{11}$$

which may be obtained by the integration by parts of the rate equations. The relationships read

$$I_{\mathrm{p-Ps}} = \lambda_{\mathrm{p-Ps}}[(1-\zeta)\mathcal{L}_1(0) + \zeta\mathcal{L}_2(0)] \tag{12}$$

$$I_{\mathrm{po}} = \lambda_{\mathrm{po}}[(1-\zeta)\mathcal{L}_2(0) + \zeta\mathcal{L}_1(0) + \mathcal{L}_3(0) + \mathcal{L}_4(0)] \tag{13}$$

$$I_{\mathrm{f}} = \lambda_{\mathrm{f}}\mathcal{L}_0(0) \tag{14}$$

where $\lambda_{\mathrm{p-Ps}}$, λ_{po}, and λ_{f} are the annihilation rates of p-Ps, o-Ps (pick-off annihilation), and of the free positrons. The sum over the time-integrated occupation numbers is independent of the magnetic field and equals the mean positron lifetime $\overline{\tau}$, i.e. the weighted sum of the lifetimes $\tau_{\mathrm{p-Ps}}$, τ_{po}, and τ_{f}. Hence we have

$$\overline{\tau} := \tau_{\mathrm{p-Ps}}I_{\mathrm{p-Ps}} + \tau_{\mathrm{po}}I_{\mathrm{po}} + \tau_{\mathrm{f}}I_{\mathrm{f}} = \mathcal{L}_0(0) + \mathcal{L}_1(0) + \mathcal{L}_2(0) + \mathcal{L}_3(0) + \mathcal{L}_4(0). \tag{15}$$

The dependence of the annihilation fractions on the magnetic field strength in terms of the reduced field x is given by

$$I_l = \frac{b_0^{(l)} + b_1^{(l)} r\mathcal{P}x + b_2^{(l)}x^2}{c_0' + c_2'x^2} \tag{16}$$

where l stands for p-Ps, po, or f. The coefficients $b_0^{(l)}$, $b_1^{(l)}$, $b_2^{(l)}$, c_0', and c_2' depend on the electron density parameter κ, on the annihilation rates $\lambda_{\mathrm{p-Ps}}$, $\lambda_{\mathrm{o-Ps}}$, and λ_{po}, and on rates characterizing the 'chemical' transition processes mentioned above [18].

3. Experimental set-up and data analysis

The Stuttgart e^+SR set-up employs spin-polarized positrons from a ^{68}Ge/^{68}Ga source with a current activity of about 1 mCi (=3.7×10^7 Bq). ^{68}Ge (half-life 275 days) decays by electron capture into ^{68}Ga (half-life 68 min). The positrons emitted in the β-decay of ^{68}Ga possess a maximum kinetic energy of 1.9 MeV, a most probable kinetic energy of 0.99 MeV, and an average kinetic energy of 0.81 MeV. This corresponds to a mean helicity $\langle\mathcal{H}\rangle = 0.92$. Static external magnetic fields $\boldsymbol{B}$ up to 2.6 T are provided by an iron-core magnet. The set-up has rotational symmetry around the $\boldsymbol{B}$-direction; hence it is natural to use this direction for defining the spin polarization according to (9). Since the positrons implanted into the sample are those emitted into a cone of half-opening angle φ, the spin polarization of the implanted positron ensemble is given by

$$\mathcal{P} = \langle\mathcal{H}\rangle \cos^2(\varphi/2). \tag{17}$$

It decreases with increasing B because of the dependence of φ on the magnetic field strength B.

The annihilation quanta are detected by a high-purity Ge detector placed about 0.7 m from the sample. Annihilation events outside the sample are eliminated by a veto detector system. The Doppler-broadened 511 keV photon line is recorded at different magnetic field strengths with count rates of about 500 counts s^{-1}; the direction of $\boldsymbol{B}$ is reversed every 5×10^3 s. A reference for software stabilization of the energy spectra is provided every

600 s by monitoring the 497 keV photon line of ^{103}Ru. This line is also used to determine the Gaussian width $\sigma_{\rm res}$ of the resolution function, which is obtained by fitting

$$G_{\rm ref} = \frac{N^{\rm res}}{\sigma_{\rm res}\sqrt{2\pi}} \exp\left[-\frac{(\Delta E_\gamma)^2}{2\sigma_{\rm res}^2}\right] \tag{18}$$

to the 497 keV line. In (18), ΔE_γ is the deviation of the photon energy from the centres of the 497 keV or 511 keV line. For further details see [10, 29].

As a measure of the relative difference between the Doppler-broadened line shapes at the two directions of the applied magnetic field an energy-integrated polarization parameter P^* is introduced as follows. The numbers of counts recorded in each channel at the two field directions are divided by the total number of counts in a suitably chosen normalization range (see figure 1(a)). The dimensionless parameter $P^* = P^*(B)$ is obtained by subtracting the two normalized spectra channel by channel and summing over a range of channels as indicated in figure 1(b). Note that P^* is an integrated quantity with respect not only to the energy but also to the positron ages.

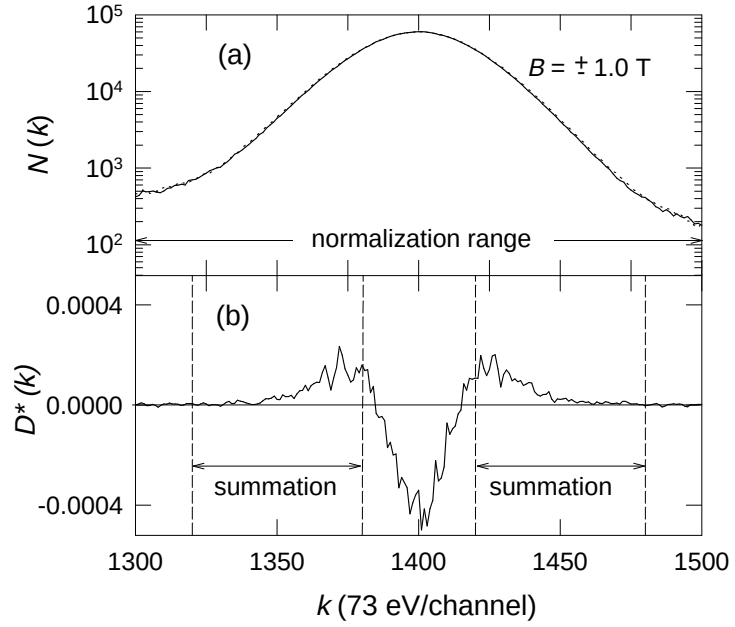

Figure 1. (a) Doppler broadening of the 511 keV line in fused quartz recorded at opposite field directions ($B = \pm 1$ T). On the scale of the diagram the two lines almost coincide. The marked channel range is used for normalization (see the text). (b) The normalized difference spectrum D^*; P^* is obtained by summation over the indicated energy ranges.

From the *time-integrated intensities* I_l (see (16)) a model function

$$P^*_{\rm model}(x) = f_{\rm po}\left[I_{\rm po}(-x) - I_{\rm po}(x)\right] + f_{\rm p-Ps}\left[I_{\rm p-Ps}(-x) - I_{\rm p-Ps}(x)\right] \tag{19}$$

for P^* may be derived, where $\pm x$ indicate the opposite field directions. The dimensionless quantities $f_{\rm p-Ps}$ and $f_{\rm po}$ are the fractions of the measured 2γ self-annihilation and pick-off annihilation events in the summation range. The summation range is chosen in such a way that if all Ps 'atoms' are thermalized, i.e., if the Ps momentum distribution is very narrow, only pick-off annihilation contributes to P^*. In this case we have $f_{\rm p-Ps} = 0$; hence $P^* \geqslant 0$

owing to $I_{\mathrm{po}}(-x) \geqslant I_{\mathrm{po}}(x)$. However, if non-thermalized Ps is present ($f_{\mathrm{p-Ps}} > 0$), P^* may become negative.

The derivation of model functions describing the *Doppler broadening* of the annihilation photon line has to start from the probability $w(p_{\mathrm{l}})\ \mathrm{d}p_{\mathrm{l}}$ that an annihilating particle has a longitudinal projection of its momentum vector $\boldsymbol{p}$ onto the direction of observation that lies between p_{l} and $p_{\mathrm{l}} + \mathrm{d}p_{\mathrm{l}}$. For the longitudinal momenta of thermalized positrons not bound in Ps we assume a probability density

$$w_{\mathrm{f}}(p_{\mathrm{l}}) = \frac{1}{\sigma_{\mathrm{f}}^*\sqrt{2\pi}} \exp\left[-\frac{p_{\mathrm{l}}^2}{2(\sigma_{\mathrm{f}}^*)^2}\right] \tag{20}$$

with Gaussian width σ_{f}^*. In order to derive a model function, $w_{\mathrm{f}}(p_{\mathrm{l}})$ has to allow for the limited energy resolution of the detector.

The model function for the contribution of the annihilation of free positrons to the 511 keV photon line is then given by

$$C_{\mathrm{f}}(p_{\mathrm{l}}; x) = \frac{N_0 I_{\mathrm{f}}(x)}{\sigma_{\mathrm{f}}\sqrt{2\pi}} \exp\left[-\frac{p_{\mathrm{l}}^2}{2\sigma_{\mathrm{f}}^2}\right] \tag{21}$$

with

$$(\sigma_{\mathrm{f}})^2 = (\sigma_{\mathrm{f}}^*)^2 + (\sigma_{\mathrm{res}})^2. \tag{22}$$

For monoenergetic Ps atoms with momentum vectors $\boldsymbol{p}_{\mathrm{Ps}}$ isotropically distributed in space, the probability density $w_{\mathrm{Ps}}(p_{\mathrm{l}})$ is given by [21]

$$w_{\mathrm{Ps}}(p_{\mathrm{l}}) = \begin{cases} 1/(2p_{\mathrm{Ps}}) & (|p_{\mathrm{l}}| \leqslant p_{\mathrm{Ps}}) \\ 0 & (|p_{\mathrm{l}}| > p_{\mathrm{Ps}}). \end{cases} \tag{23}$$

The model function for the Ps contribution to the 511 keV photon line has to allow not only for the limited energy resolution but also for the distribution of the momenta of pick-off electrons. We assume that this distribution is adequately represented by the probability density

$$w_{\mathrm{po}}(p_{\mathrm{l}}) = \frac{1}{\sigma_{\mathrm{po}}^*\sqrt{2\pi}} \exp\left[-\frac{p_{\mathrm{l}}^2}{2(\sigma_{\mathrm{po}}^*)^2}\right] \tag{24}$$

with Gaussian width σ_{po}^*. The momentum probability density for Ps is then obtained by convoluting (23) with the resolution function of the detector and, in the case of o-Ps, additionally with (24). This leads to

$$w_i(p_{\mathrm{l}}) = \frac{1}{4a_i p_{\mathrm{Ps}}}\left[\mathrm{erf}\left(\frac{p_{\mathrm{l}} + a_i p_{\mathrm{Ps}}}{\sqrt{2}\sigma_i}\right) - \mathrm{erf}\left(\frac{p_{\mathrm{l}} - a_i p_{\mathrm{Ps}}}{\sqrt{2}\sigma_i}\right)\right] \tag{25}$$

where i stands for p-Ps or po; the dimensionless factors a_i weigh the influence of the Ps momenta p_{Ps} on $w_i(p_{\mathrm{l}})$. Whereas $a_{\mathrm{po}} = 1/2$ since in pick-off annihilations only the positrons take part, in self-annihilations both Ps constituents, electron and positron, contribute their moments to $w_i(p_{\mathrm{l}})$; hence $a_{\mathrm{p-Ps}} = 1$. The widths σ_i appearing in (25) are given by

$$(\sigma_{\mathrm{p-Ps}})^2 = (\sigma_{\mathrm{p-Ps}}^*)^2 + (\sigma_{\mathrm{res}})^2 \tag{26a}$$

or

$$(\sigma_{\mathrm{po}})^2 = (\sigma_{\mathrm{po}}^*)^2 + (\sigma_{\mathrm{res}})^2 \tag{26b}$$

depending on whether we consider p-Ps or o-Ps; in (26*a*) we introduced the width $\sigma_{\mathrm{p-Ps}}^*$ to allow for a Doppler shift of the photon energies in the 2γ self-annihilation of Ps.

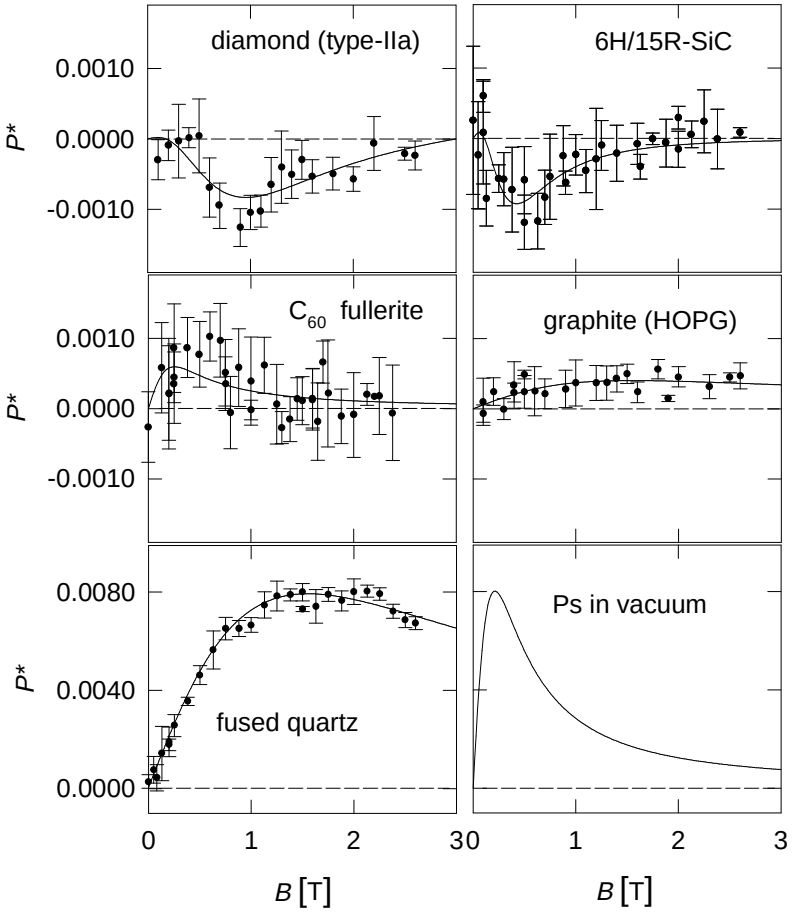

Figure 2. The dependence of P^* on the strength of the applied magnetic field B as measured at room temperature on natural (type-IIa) diamond, crystalline SiC (6H/15R polytype), graphite (HOPG), fused quartz (SUPRASIL), and C_{60} fullerite; the solid lines are the results of fits to the data. The curve for Ps in vacuum has been calculated.

In the case of *thermalized* Ps, p_{Ps} is independent of the e^+ age and small enough for (25) to be replaced by Gaussians. The contributions to the 511 keV photon line due to the annihilation of Ps are then given by

$$C_i(x;\, p_{\mathrm{l}}) = \frac{N_0 I_i(x)}{\sigma_i\sqrt{2\pi}} \exp\left[-\frac{p_{\mathrm{l}}^2}{2\sigma_i^2}\right] \qquad i = \text{p-Ps, po.} \tag{27}$$

For *non-thermalized* Ps, p_{Ps} depends on the positron age according to (4). In this case the quadrature of (25) with respect to t was carried out numerically.

If the background in the energy spectra is described by two functions $U_0(\Delta E_\gamma; x)$ and $U_1(\Delta E_\gamma; x)$ as outlined in [18], the number of counts in the energy range used in the analysis may be represented by the sum

$$N_{\mathrm{model}}(\Delta E_\gamma; x) = G_{\mathrm{ref}} + \sum_l C_l + U_0 + U_1 \qquad l = \text{p-Ps, po, f.} \tag{28}$$

Since the experiment measures the Doppler shifts ΔE_γ, the contributions C_l, which

according to (27) depend on the momentum p_l, have to be transformed to ΔE_γ-dependent functions by means of (2).

The full information content of the experimental data is used in a simultaneous least-squares fit of the model functions (19) and (28) to the magnetic field dependence of the polarization parameter P^* and of the 511 keV photon line shape. This gives us numerical values for the fraction r of Ps-forming positrons, the electron density parameter κ, the pick-off annihilation rate λ_{po}, and the width σ^*_{po} characterizing the momentum distribution of the pick-off electrons, plus additional parameters depending on whether we include non-thermalized Ps or not. For thermalized Ps the contributions C_i (see (27)) have been used with the Gaussian width σ^*_{p-Ps} as fit parameter. If non-thermalized Ps is present, C_{p-Ps} and C_{po} are derived by integrating (25) with respect to t. In this case the fit parameters are the kinetic energy E_0 at the instant of Ps formation and the Ps slowing-down time τ_{sd}.

Table 1. Characteristic parameters of Ps in natural type-IIa diamond, crystalline SiC (6H/15R polytype), and fused quartz (SUPRASIL): the fraction of Ps-forming e^+, r; the electron density parameter, κ; the pick-off lifetime, $\tau_{po} = (\lambda_{po})^{-1}$; the slowing-down time, τ_{sd}; the kinetic energy, E_0, at the time of Ps formation; and the Gaussian width, σ^*_{po}, characterizing the momentum distribution of pick-off electrons. The deformation potential E_{op} is derived from relation (5) by inserting the mass densities ρ listed in the table

	Diamond (type-IIa)	SiC (6H/15R polytype)	Fused quartz (SUPRASIL)
r	0.07 ± 0.01	0.037 ± 0.004	0.67 ± 0.04
κ	0.99 ± 0.05	0.15 ± 0.02	1.4 ± 0.1
τ_{po} (10^{-9} s)	31 ± 7	20 ± 8	1.6 ± 0.1
τ_{sd} (10^{-9} s)	12.6 ± 0.6	9 ± 2	0.04 ± 0.01
E_0 (eV)	8.03 ± 0.06	6.85 ± 0.07	3.08 ± 0.08
σ^*_{po} (keV)	2.1 ± 0.3	1.8 ± 0.2	1.07 ± 0.03
E_{op} (10^{10} eV m^{-1})	0.07	0.08	0.83
ρ (g cm^{-3})	3.52	3.21	2.25

4. Results

Room temperature e^+SR measurements were performed on fused quartz (SUPRASIL), natural type-IIa diamond (the same sample as was studied in [37]), crystalline SiC (6H/15R polytype), highly orientated pyrolytic graphite (HOPG), and purified C_{60}/C_{70} fullerite powder (C_{60} content about 0.8 M, mean crystallite size about 2 μm). The fullerite powder was compacted to disk-shaped pellets (diameter 8 mm, thickness about 3 mm) at a pressure of about 20 MPa.

Figure 2 contrasts the dependence of P^* on the applied field B as derived by the data-handling procedure described in section 3 with $P^*(B)$ as calculated for Ps at rest in vacuum and normalized to the same maximum value $\hat{P}^*$ as that of fused quartz. The vanishing of P^* at low magnetic fields is trivial. The tendency of P^* to go to zero at high magnetic field strengths is in agreement with the fact that in the regime $B \gg \Delta E^{hf}/\mu_e$ positron and electron spins are decoupled and that, as a consequence, the occupation numbers of the energy eigenstates of Ps contributing to the 2γ self-annihilation and to the pick-off annihilation become independent of the field direction. Thus, in Ps-forming materials, P^*

must show at least one extremum as a function of B. Apart from this common feature, the $P^*(B)$ curves of figure 2 are very different. This will be discussed in section 5. The solid lines in figure 2 represent the results of simultaneous least-squares fits to the magnetic field dependences of P^* and to the 511 keV photon line shape (cf. section 3). The fit parameters are listed in table 1 (materials with evidence for non-thermalized Ps) and table 2 (materials without evidence for non-thermalized Ps)

Table 2. Ps fractions r, electron density parameters κ, and pick-off lifetimes $\tau_{po} = (\lambda_{po})^{-1}$ of positronium in graphite (HOPG) and C_{60} fullerite.

	Graphite (HOPG)	C_{60} fullerite
r	0.009 ± 0.006	0.03 ± 0.01
κ	0.7 ± 0.1	0.3 ± 0.1
τ_{po} (10^{-9} s)	0.56 ± 0.03	25 ± 10
σ^*_{p-Ps} (keV)	0.4 ± 0.2	0.5 ± 0.3
σ^*_{po} (keV)	3.1 ± 1.3	2.8 ± 1.4

5. Discussion

In the comparison of the experimental data with the calculated $P^*(B)$ and in their qualitative interpretation, the answers to the following three questions are very helpful.

(i) Is the absolute magnitude of $P^*(B)$ at its extremum, $|\hat{P}^*|$, comparable with or much smaller than that of strong Ps formers (in the present case, fused quartz, which was among the first solids in which Ps was identified [31])?

(ii) Is P^* positive or negative?

(iii) At which magnetic field does $P^*(B)$ reach its extremum?

From the answers we may draw the following conclusions.

(i) If $|\hat{P}^*|$ is small compared with the corresponding values for strong Ps formers, the positronium yield r is small compared with unity (figure 2: graphite, C_{60} fullerite).

(ii) Negative P^*-values can result only if, on average, the momenta of self-annihilating p-Ps or p-Ps-like (e^+e^-) systems are larger than those of the electrons contributing to pick-off annihilation (cf. (19)). They are therefore a very strong and, as the examples of diamond and SiC show, quite sensitive indication of Ps formation. Moreover, negative P^*-values are a sufficient indicator (but not a necessary one—see fused quartz) for the annihilation of an appreciable fraction of p-Ps with *epithermal* kinetic energies.

(iii) $\hat{B}$ shifts to higher values with increasing κ but is also strongly influenced by λ_{po} (for details see [8]). A $\hat{B}$-value very much larger than the vacuum value $B_{vac} = 0.22$ T indicates that $\kappa > 1$. The tentative conclusion from figure 2 that the κ-value of fused quartz might exceed unity (which means a stronger overlap of the e^+ and e^- wavefunctions than in isolated positronium) has been confirmed by the quantitative analysis of the data (cf. table 1) and by lifetime measurements in applied magnetic fields on the same sample [30]. We conclude that in fused quartz the action of local electric fields, which tend to separate electrons and positrons in positronium, is overcompensated by the Pauli (exchange) repulsion of the electron by its neighbours.

Ps formation in graphite and C_{60} fullerite, for which the e^+SR measurements gave very small yields ($r = 0.01$ or 0.03, respectively), has so far not been detected by e^+ lifetime measurements [32, 33]. For the detection of small Ps yields such measurements are indeed less suited than e^+SR investigations. The electron density parameter of graphite, $\kappa = 0.7$, is larger than that of C_{60} fullerite, $\kappa = 0.3$, whereas the pick-off lifetime in C_{60} fullerite $\tau_{po} = 25 \times 10^{-9}$ s exceeds by far that in graphite ($\tau_{po} = 0.56 \times 10^{-9}$ s). This may be understood if in graphite Ps is formed in the spacings between adjacent carbon layers and in C_{60} fullerite in the interior of the C_{60} molecules. The distance between the planes in graphite is 3.35×10^{-10} m and the diameter of a C_{60} molecule is 7.1×10^{-10} m; thus the spatial overlap between positron and electron wavefunctions and therefore the value of κ should be larger in graphite. In C_{60} fullerite the electron density is very low in the interior of the C_{60} molecules [34], so a small Ps formation probability and a long pick-off lifetime is expected for Ps residing inside the molecules.

Ps formation outside the C_{60} molecules would presumably require chemical bonding of the Ps atom to the surface of the C_{60} molecule. Lifetime measurements [33] led to the conclusion that positrons in C_{60} fullerite annihilate with a lifetime of about 0.4×10^{-9} s predominantly at sites between the C_{60} molecules; since this lifetime is less than the 'low-density limit' $\tau_\infty = 500$ ps of the e^+ lifetime in a gas of conduction electrons [35], it is presumably due to 'free' e^+ and not to Ps in the intermolecular region.

The data on natural type-IIa diamond and crystalline SiC show the novel feature that P^* is negative. As explained above, the dependence of the polarization parameter P^* on the magnetic field indicates clearly the presence of p-Ps or Ps-like (e^+e^-) systems, the decrease of P^* towards zero at high magnetic field strength being attributed to the 'quenching' of the hyperfine interaction between the magnetic moments of the positron and electron. Since negative values of the polarization parameter P^* can be found only if the Ps momenta are considerably larger than that of pick-off electrons, an appreciable fraction of Ps in natural diamond and crystalline SiC has not yet thermalized at the time of annihilation.

Positronium in natural diamond was found earlier by combined 2D-ACAR and positron lifetime measurements and ascribed to Ps formation in grain boundaries [36]. On the other hand, in lifetime measurements on the sample investigated in the present e^+SR experiments positronium was *not* detected; it was concluded that all positrons annihilate as e^+ either in the bulk or in lattice vacancies [37].

To our knowledge, positronium in crystalline SiC has not yet been reported, possibly because the formation probability $r = 0.037$ was too small to allow detection by one of the conventional techniques such as ACAR or lifetime measurements.

For both materials, natural diamond and crystalline SiC, the dependence of P^* on the magnetic field strength could be fitted in a satisfactory manner only by taking the annihilation of non-thermalized positronium into consideration. The initial Ps kinetic energies $E_0 \approx 8$ eV in natural diamond and $E_0 \approx 7$ eV in crystalline SiC resulting from the fit are comparable to the Ps binding energy in vacuum, $E_B = 6.8$ eV, and thus quite plausible. Surprisingly, the slowing-down times exceed the usual pick-off lifetimes in condensed matter ($\tau_{po} = 1$–5 ns) by far (cf. table 1). If τ_{sd} is expressed in terms of the deformation potential E_{op}, one finds that it is one order of magnitude smaller than in fused quartz (cf. table 1) or some organic liquids such as methanol [21]. Our analysis led to pick-off lifetimes $\tau_{po} = 31$ ns in diamond and $\tau_{po} = 20$ ns in SiC that are much larger than so far found in condensed matter. Since the present e^+SR technique integrates over the e^+ age, it is clearly not the best method for studying lifetimes. The outcome of future background-free lifetime measurements should be awaited before further conclusions are drawn.

The e^+SR results on fused quartz indicate that here the self-annihilation of non-

thermalized p-Ps plays a rôle, too. The initial kinetic energy $E_0 = 3.1$ eV, i.e. a value smaller than the Ps binding energy, and the slowing-down time $\tau_{sd} = 40$ ps, agree reasonably well with the results of a recent analysis [21] of AMOC experiments on fused quartz [38].

6. Conclusions

The positron spin-relaxation (e^+SR) technique is a powerful tool for the study of positronium in condensed matter. Its strength is the detection and quantitative study of small positronium yields that may not be accessible by lifetime measurements.

At room temperature small Ps-forming fractions of implanted e^+ could be found in graphite ($r \approx 0.01$) and in C_{60} fullerite ($r = 0.03$). The electron density parameter κ and the pick-off rate λ_{po} are significantly smaller in C_{60} fullerite ($\kappa = 0.3$, $\lambda_{po} = 0.04 \times 10^9$ s^{-1}) than in graphite ($\kappa = 0.7$, $\lambda_{po} = 1.8 \times 10^9$ s^{-1}).

In natural diamond and crystalline SiC experimental evidence was found not only for the existence of Ps but also for the annihilation of non-thermalized positronium, characterized by the slowing-down time τ_{sd} and the Ps kinetic energies E_0 at the instant of Ps formation. For diamond $r = 0.07$, $\tau_{sd} = 13 \times 10^{-9}$ s, $E_0 \approx 8$ eV, and for SiC $r = 0.04$, $\tau_{sd} = 20 \times 10^{-9}$ s, and $E_0 \approx 6.9$ eV were found.

For fused quartz, the parameters characterizing Ps turned out to be $r = 0.67$, $\kappa = 1.4$, $\lambda_{po} = 0.63 \times 10^9$ s^{-1}, $E_0 \approx 3$ eV, and $\tau_{sd} = 0.04 \times 10^{-9}$ s.

Acknowledgments

The authors would like to thank Dr S H Connell (University of Witwatersrand, South Africa) for making available the diamond sample and Dr R Scheuermann (Universität Stuttgart, Germany) for providing us with the C_{60} fullerite. Particular thanks are due to Dr I Billard (Centre de Recherches Nucléaires, Strasbourg, France) for the investigation of fused quartz by lifetime measurements and to Dr P Harmat (Research Institute for Technical Physics and Materials Science, Budapest, Hungary) for developing the data acquisition system and the veto detector part of the experimental set-up. The help of Dr C Ulrich (Max-Planck-Institut für Festkörperforschung, Stuttgart, Germany), who characterized the SiC sample by Raman spectroscopy, is gratefully acknowledged. We are also indebted to Drs P Castellaz, A Siegle, and H Stoll (Max-Planck-Institut für Metallforschung) for helpful discussions and to R Henes, P Keppler, and W Maisch (Max-Planck-Institut für Metallforschung) for preparing the SiC sample.

References

[1] Seeger A 1984 *Muons and Pions in Materials Research* ed J Chappert and R I Grynszpan (Amsterdam: North-Holland) p 251
[2] Schenck A 1985 *Muon Spin Rotation Spectroscopy* (Bristol: Hilger)
[3] Smilga V P and Belousov Yu M 1994 *The Muon Method in Science* (New York: Nova Science)
[4] Kubica P and Stewart A T 1975 *Phys. Rev. Lett.* **34** 852
[5] Lee-Whiting G E 1955 *Phys. Rev.* **97** 1557
[6] Jensen K O and Walker A B 1990 *J. Phys.: Condens. Matter* **2** 9757
[7] Akahane T and Berko S 1982 *Positron Annihilation* ed P G Coleman, S Sharma and L M Diana (Amsterdam: North-Holland) p 874
[8] Major J, Seeger A, Ehmann J and Gessmann Th 1997 *Positronium in Condensed Matter Studied with Spin-Polarized Positrons (Lecture Notes in Physics 499)* ed K Jungmann, J Kowalski, I Reinhard and F Träger (Berlin: Springer) p 381

[9] Seeger A, Major J and Jaggy F 1985 *Positron Annihilation* ed P C Jain, R M Singru and K P Gopinathan (Singapore: World Scientific) p 137
[10] Seeger A, Major J and Banhart F 1987 *Phys. Status Solidi* a **102** 91
[11] Banhart F, Major J and Seeger A 1989 *Positron Annihilation* ed L Dorikens-Vanpraet, M Dorikens and D Segers (Singapore: World Scientific) p 281
[12] Deckers Ch, Ehmann J, Greif H, Keuser F, Knichel W, Lauff U, Maier K, Siegle A and Tongbhoyai M 1995 *J. Physique Coll.* IV **5** C1 81
[13] Page L A and Heinberg M 1957 *Phys. Rev.* **106** 1220
[14] Bisi A, Consolati G, Quasso F and Zappa L 1989 *Nuovo Cimento* D **11** 635
[15] Seeger A 1998 to be published
[16] Berko S and Pendleton H P 1980 *Annu. Rev. Nucl. Part. Sci.* **30** 543
[17] Consolati G 1996 *J. Radioanalyt. Nucl. Chem., Articles* **210** 273
[18] Gessmann Th, Harmat P, Major J and Seeger A 1997 *Z. Phys. Chem., NF* **199** 213
[19] Seeger A 1995 *Appl. Surf. Sci.* **85** 8
[20] Nieminen R M and Oliva J 1980 *Phys. Rev.* B **22** 2226
[21] Siegle A 1997 Positronenzerstrahlung in kondensierter Materie–eine Untersuchung mit der Methode der Lebensalter-Impuls–Korrelation *Dr Rer. Nat. Thesis* Stuttgart University
[22] Billard I, Abbé J Ch and Duplâtre G 1991 *J. Chem. Phys.* **95** 2501
[23] Castellaz P, Major J, Mujica C, Schneider H, Seeger A, Siegle A, Stoll H and Billard I 1996 *J. Radioanalyt. Nucl. Chem., Articles* **210** 457
[24] Goldanskii V I and Prokopev E P 1996 *JETP Lett.* **4** 284
[25] Dupasquier A 1983 *Positron Solid-State Physics* ed W Brandt and A Dupasquier (Amsterdam: North Holland) p 510
[26] Zitzewitz P W, Van House J C, Rich A and Gidley D W 1979 *Phys. Rev. Lett.* **43** 1281
[27] Gidley D W, Köymen A R and Weston Capehart T 1982 *Phys. Rev. Lett.* **49** 1779
[28] Rich A, Van House J, Gidley D W, Conti R S and Zitzewitz P W 1987 *Appl. Phys.* A **43** 275
[29] Gessmann Th, Harmat P, Major J and Seeger A 1997 *Appl. Surf. Sci.* **116** 114
[30] Billard I 1996 private communication (Strasbourg)
[31] Bell R E and Graham R L 1953 *Phys. Rev.* **90** 644
[32] Jean Y C, Lu X, Lou Y, Bharathi A, Sundar C S and Lyu Y 1992 *Phys. Rev.* B **45** 12 126
[33] Schaefer H-E, Forster M and Würschum R 1992 *Phys. Rev.* B **45** 12 164
[34] Puska M J and Nieminen R M 1992 *J. Phys.: Condens. Matter* **4** L149
[35] Seeger A and Banhart F 1987 *Phys. Status Solidi* a **102** 171
[36] Fujii S, Nishibayashi Y, Shikata S, Uedono A and Tanigawa S 1995 *J. Appl. Phys.* **78** 1510
[37] Nilen R W N, Lauff U, Connell S H, Stoll H, Siegle A, Schneider H, Castellaz P, Kraft J, Bharuth-Ram K, Sellschop J P F and Seeger A 1997 *Appl. Surf. Sci.* **116** 198
[38] Schneider H, Seeger A, Siegle A, Stoll H, Castellaz P and Major J 1997 *Appl. Surf. Sci.* **116** 146